Enhanced-Range Intrusion Detection Using Pyroelectric Infrared (PIR) Sensors

Sami Aldalahmeh[1,†], Amer M. Hamdan[1,†], Mounir Ghogho[2,3,‡] and Des McLernon[2,‡]

[1]Al-Zaytoonah University of Jordan, Jordan, [2]Leeds University, UK, [3]International University of Rabbat, Morocco.

[†]{s.aldalahmeh, a.hamdan}@zuj.edu.jo,[‡]{m.ghogho, d.c.mclernon}@leeds.ac.uk.

1. Abstract

Intrusion detection using *pyroelectric infrared sensors* (PIR) is investigated in the light of the geometry of intruder's trajectory. The PIR signal is modeled by a sum of exponentially modulated sinusoids. Consequently, the intrusion detection is formulated as a hypothesis testing problem and we propose an exponentially windowed periodogram (EWP) detector also able to estimate the direction of movement. Simulation results show superior EWP performance when compared to the periodogram detector and the energy detector over large distances. Results show nearly 100% correct detection of the direction of movement.

2. Introduction

- PIR sensors are crystals that produces a voltage when exposed to temperature change, enabling motion detection.
- Two sensor elements are cascaded in reverse polarity producing an alternating pulse when the intruder moves across field of view (FOV).
- Due to relatively low detection range the outdoor applications are limited.
- Therefore, advanced processing techniques are needed in order to increase the detection range of the PIR sensors.

Variable	Meaning	Variable	Meaning
Φ	Heat flux	A_s	Sensor's surface area
ε	Intruder's emissivity	$\omega_{i,s}$	Solid projected angle
k_B	Steveman-Boltzmann const	R	Intruder-sensor separation
T_i	Intruder's temperature	v	Intruder's speed
T_s	Sensor's temperature	t_i	Entry time of ith FOV
A_i	Intruder's surface area	d_i	Segment lenght of ith FOV

Table 1: *Variables*

3. Modeling of Intruder's Signature

3.1 Intruder Heat Flux

- The intruder is assumed to be Lambertian grey body [1] moving with constant speed.
- The intruder emits heat flux uniformly in space. The heat flux at the sensor is given by eq. (1).
- $\omega_{i,s}$ is the projected solid angle of the intruder onto the sensor usually found by a finite element method (FEM), which is difficult to compute.
- For relatively moderate intruder-sensor separation (R), eq. (2) provides an accurate approximation of (1) as shown in Fig. 1.

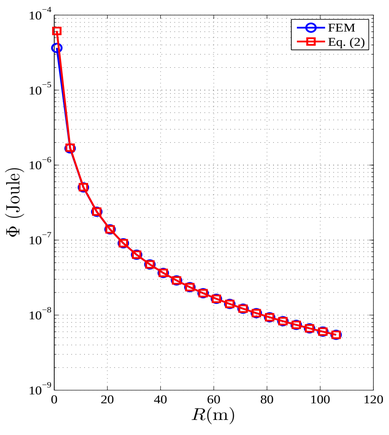

$$\Phi = \frac{1}{\pi}\varepsilon k_B \omega_{i,s}\left(T_i^4 - T_s^4\right) A_i \tag{1}$$

$$\Phi \approx \varepsilon k_B \left(T_i^4 - T_s^4\right)\frac{A_i A_s}{4R^2} \tag{2}$$

Figure 1: Φ *as a function of* R.

- For an intruder moving in a straight line with constant speed v, crossing the FOVs of the sensor, as shown in Figs. 2, the trajectory is shown in Fig. 3.
- The resulting heat flux is given in eq. (3)

$$\Phi(t) = \frac{\tilde{\Phi}}{R^2(t)}\sum_{i=-F}^{F}\left[\Pi\left(\frac{t-t_i}{d_i^+/v}\right) - \Pi\left(\frac{t-t_i-d_i^+/v}{d_i^-/v}\right)\right] \tag{3}$$

$$R^2(t) = v^2t^2 + \frac{2vR_0\sin\psi_0}{\tan(\psi_0+\gamma)}t + \left(\frac{R_0\sin\psi_0}{\sin(\psi_0+\gamma)}\right)^2 \tag{4}$$

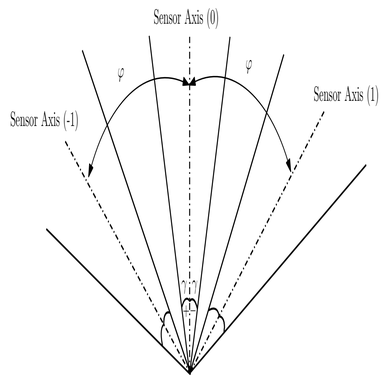

Figure 2: *Multi-segment Frensel lens.*

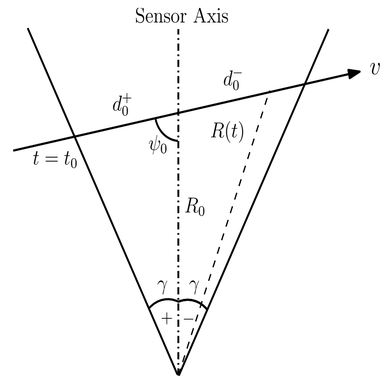

Figure 3: *Intruder crossing FOV.*

3.2 PIR Signal

- The PIR sensor acts as a bandpass filter with transfer function [1, 3]

$$H(s) = \frac{Ks}{(1+\tau_1 s)(1+\tau_2 s)} \tag{5}$$

where K is the gain and τ_1 and τ_2 are the thermal and electrical time constants respectively.
- Thus the PIR voltage generated is $s(t) = \Phi(t) * h(t)$.
- Noise is added to the signal giving the measured signal $x(t) = s(t) + w(t)$ where $w(t)$ is zero mean AWGN with variance σ^2.
- For an intruder moving away from sensor, the heat flux is in Fig. 4 the PIR signal is shown in Fig. 5.

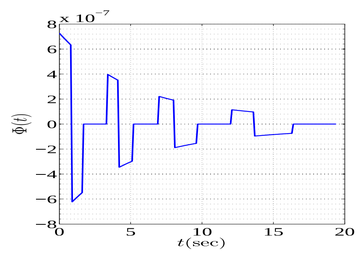

Figure 4: *Heat flux of intruder.*

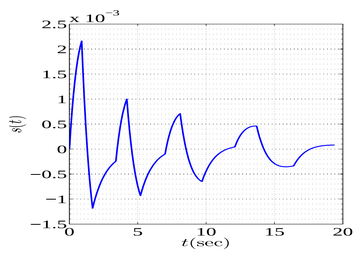

Figure 5: *PIR voltage signal.*

- For an intruder moving towards the sensor, the heat flux is in Fig. 6 the PIR signal is shown in Fig. 7.

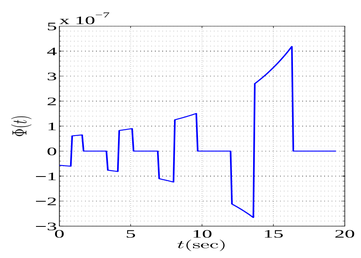

Figure 6: *Heat flux of intruder.*

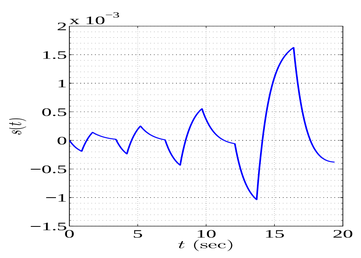

Figure 7: *PIR voltage signal.*

4. Intrusion Detection

- Given appropriate sampling, the intrusion detection problem is formulated as the following hypothesis testing problem

$$\begin{aligned}\mathcal{H}_0 &: x[n] = w[n]\\ \mathcal{H}_1 &: x[n] = s[n] + w[n].\end{aligned} \tag{6}$$

- The PIR signal can be approximated as a sum of decaying sinusoids:

$$s[n] = \sum_{i=0}^{L-1}\alpha^n\left[a_i\cos(2\pi f_i n) + b_i\sin(2\pi f_i n)\right]. \tag{7}$$

Lumping the unkown parameters into vector $\boldsymbol{\theta} = (\alpha, f_0, \cdots, f_{L-1})^T$, the detection problem in vector format is:

$$\begin{aligned}\mathcal{H}_0 &: \mathbf{x} = \mathbf{w}\\ \mathcal{H}_1 &: \mathbf{x} = \mathbf{G}(\boldsymbol{\theta})\mathbf{c} + \mathbf{w}\end{aligned} \tag{8}$$

where $\mathbf{c} = (a_0, \cdots, a_{L-1}, b_0, \cdots, b_{L-1})^T$, $\mathbf{g}_c(\alpha, f_i) = \left(1, \alpha\cos(2\pi f_i), \cdots, \alpha^{N-1}\cos(2\pi f_i(N-1))\right)^T$, $\mathbf{G}(\boldsymbol{\theta}) = (\mathbf{g}_c(\alpha, f_0), \cdots, \mathbf{g}_c(\alpha, f_{L-1}), \mathbf{g}_s(\alpha, f_0), \cdots, \mathbf{g}_s(\alpha, f_{L-1}))^T$, and $\mathbf{g}_s(\alpha, f_i) = \left(0, \alpha\sin(2\pi f_i), \cdots, \alpha^{N-1}\sin(2\pi f_i(N-1))\right)^T$.

- Optimally, GLRT [2] is used. However it is computationally expensive, due to the columns of $\mathbf{G}(\boldsymbol{\theta})$ being nonorthogonal.
- We propose the EWP detector by imposing the missing orthogonality leading to the exponentially windowed periodogram

$$T_{\text{EWP}}(\mathbf{x}) = \max\frac{1}{N}\sum_{i=0}^{L-1}|X_\alpha(f_i)|^2 \tag{9}$$

where $X_\alpha(f_i) = \sum_{n=0}^{N-1}\alpha^n x[n] e^{-j2\pi f_i}$.
- EWP is able to exactly find the direction of movement. If $\hat{\alpha} > 1$ the intruder is moving away and if $\hat{\alpha} < 1$ is moving toward the sensor.

5. Simulation Results

- Using 10^5 Monte Carlo simulations, we compare three detectors: energy detector (ED), periodogram detector (PD), and EWP. The parameters used are

F	γ	v	ψ	T_i	T_s	A_i	A_s	K	τ_1	τ_2
4	7.5^o	5 kmph	50^o	37^o	20^o	0.7m^2	20μm	6000	4.2sec	1sec

Table 2: *Simulation parameters.*

- Intruder moving away from sensor.

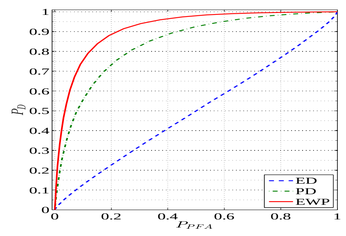

Figure 8: *ROC for* $R_0 = 50m$.

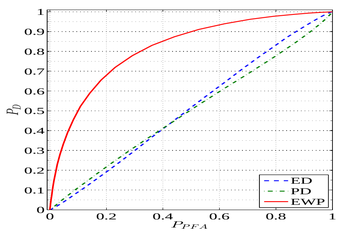

Figure 9: *ROC for* $R_0 = 90m$.

- Intruder moving towards the sensor.

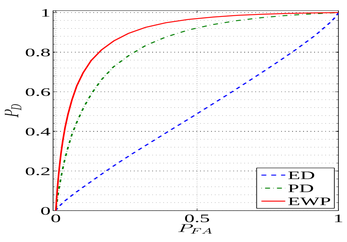

Figure 10: *ROC for* $R_0 = 50m$.

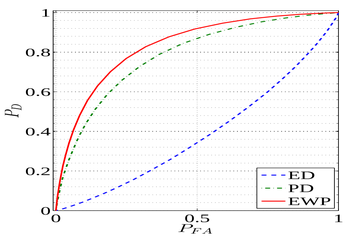

Figure 11: *ROC for* $R_0 = 90m$.

- The direction estimation results are given in the Table below.

R_0	10m	30m	50m	70m	90m
Away	100%	100%	100%	100%	100%
Toward	100%	100%	100%	100%	99.89%

Table 3: *Direction estimation*

6. Conclusions

- An inverse square-law is established relation for the incident heat flux and the separation distance.
- The PIR sensor output signal is modeled by the sum of exponentially modulated sinusoids.
- The EWP detector is proposed showing very good detection performance for long distances.

7. Acknowledgement

This research was funded by Al- Zaytoonah University of Jordan grant (8/12/2014).

References

[1] Helmut Budzier. *Thermal infrared sensors theory, optimization, and practice*. Wiley, Chichester, West Sussex, U.K. Hoboken, N.J, 2011.

[2] Steven M. Kay. *Fundamentals of Statistical Signal Processing, Volume 2: Detection Theory*. Prentice Hall, 1998.

[3] Andrzej Odon. Modelling and simulation of the pyroelectric detector using matlab/simulink. *Measurement Science Review*, 10(6):195–199, 2010.